

## Use and assessment of preliminary FE model results within testing process of offshore wind turbine supporting structure

Maciej Kahsin<sup>1</sup>, Marcin Łuczak<sup>2</sup>, Bart Peeters<sup>3</sup>

<sup>1</sup> Gdansk University of Technology, Gdansk, Poland,

<sup>2</sup> Department of Transonic Flows., Centre for Thermomechanics of Fluids, Institute of Fluid-Flow Machinery, Polish Academy of Sciences, ul. Fizyera 14, 80-231 Gdańsk, Poland

<sup>3</sup> LMS International, Interleuvenlaan 68, B-3001 Leuven, Belgium

email: mkahsin@pg.gda.pl, marcin.luczak@imp.gda.pl, bart.peeters@lmsintl.com

**ABSTRACT:** Since offshore wind turbine supporting structures are subjected to dynamic environments with time-varying loading conditions, it is important to model their dynamic behavior and validate these models by means of vibrational experiments. In this paper assessment of dynamical state of the structure is investigated by means of both: numerical modeling, and experimental modal analysis. In experimental modal analysis, capturing the real dynamic behavior of tested structure requires a proper sensors and exciters localization. It is often useful to know probable dynamical behavior of the structure before experimental campaign planning. Therefore, the initial FE model results are exploited in order to predict the best configuration for a measuring equipment placement. Acquired test results are compared with FE solutions subsequently. Such a routine allows to assess quality of the preliminary numerical model on the global level, and along with a sensitivity analysis assemble a good starting point for fine-tuning of FE model.

**KEY WORDS:** offshore wind, support structure, experimental modal analysis, correlation analysis, numerical model updating.

### 1 INTRODUCTION

The offshore wind technology is rapidly developing area. In many scenarios it is foreseen as a future of European renewable energy source. This persistently evolving technology require constant updates of knowledge database in very wide scope of disciplines. In this paper issues related to structural dynamics of the support structure are addressed.

### 2 SCOPE OF THE RESEARCH

Presented combined numerical and experimental investigations are outcomes of the first stage of the research project entitled:

*Development of the selection method of the offshore wind turbine support structure for Polish maritime areas* with acronym AQUILO. Project AQUILO is supported by a Polish National Research and Development Center under the grant PBS1/A6/8/2012. The aim of the project is to create a knowledge base, from which the investor will be able to decide on the best type of support structure for offshore wind farm specific location in Polish maritime areas. Focal point of the research is the support structure of the offshore wind turbine of the tripod type [8].

#### 2.1 Global structure overview

Design of the structure under investigation in fully assembled configuration and integration with the auxiliary measurement setup is presented on Figure 1. Model scale offshore wind turbine with support is attached to the rotary support. Rotary support is equipped with moment of force sensors for wave hydrodynamic loads on the tripod model. Rotation is required to expose investigated system at different angles against incoming waves in the rectangular, unidirectional wave basin.

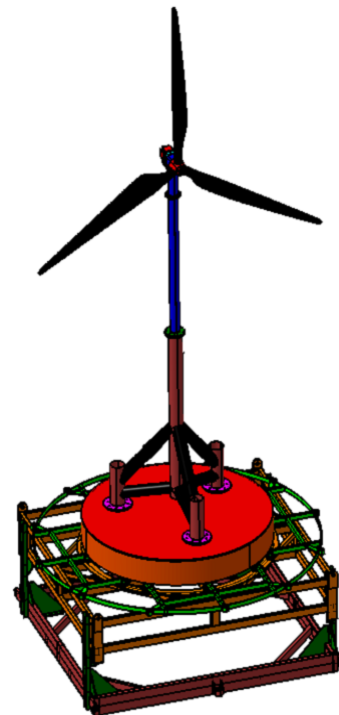


Figure 1 Geometry of the laboratory scale model of the offshore wind turbine attached to the test rig.

#### 2.2 Object of the investigation

Object of investigation was a laboratory scale model of the tripod type support structure for the offshore wind turbine. It was made of aluminum cylindrical beams. Height of the model is 2 meters and weights 30 [kg]. It comprises of three pile guides fixed to the central column with upper and lower braces (Figure 2).



Figure 2 Tripod model in experimental setup for structural dynamics identification

### 3 NUMERICAL MODEL DEVELOPMENT

As a tool of numeric analysis, Finite Element (FE) modeling technique was chosen. The simulation had to mimic two measurement campaign scenarios, one with use of acceleration sensors, and the second one with use of strain sensors. Initially only the one FE model was planned. The strain measurement campaign dictated very fine mesh composition because in this case strain field should be accurately represented. This condition was not needed in case of measurement with use of accelerometers. Considering the iteration-wise procedure employed during model updating it was decided that two mesh topologies should be prepared.

#### 3.1 Computer Aided Design geometry of the modeled structure

The original delivered geometry was prepared as a solid model. Due to the fact that assumed thickness of the structure was 3 [mm] (Figure 3), and as consequence stress along the thickness would be negligible small, the plain stress approach was applied. The solid geometry was converted to a surface model, i.e. instead of the solid geometry, the mid-surface

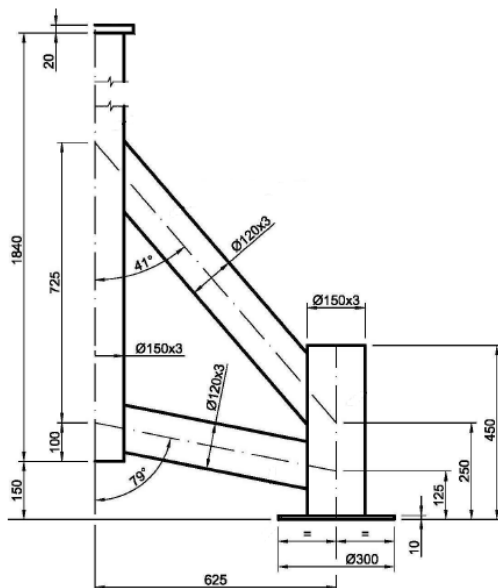


Figure 4 Dimensions of the supporting structure

model was created. Taking advantage on circular symmetry, and to reduce time of model preparation, only the cut piece spanned on an angle of 30 degrees was utilized. Furthermore, geometry was partitioned in the aim to sustain mesh regularity (Figure 4).

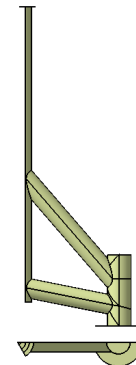


Figure 4 The mid-surface model used during FE mesh generation

#### 3.2 Finite Element Model Development

Mesh topologies developed for both measuring campaigns approaches are presented in (Figure 5).

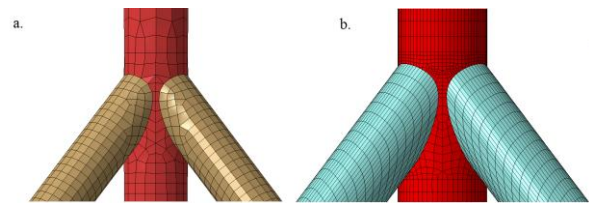


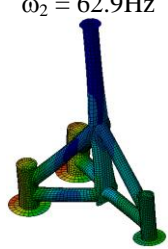
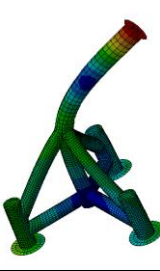
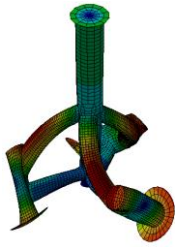
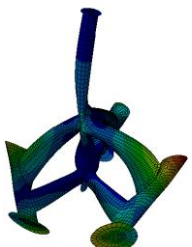
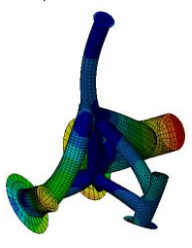
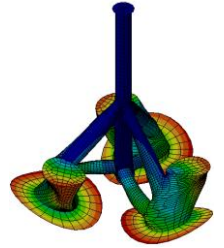
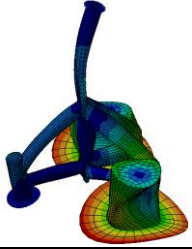
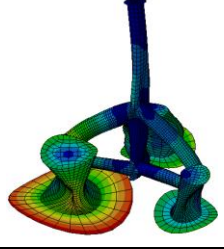
Figure 5 A sample of mesh topologies exploited in accelerometers measurements (a), and strain gauges measurements (b)

The first topology (Figure 5a) consists of 7027 nodes, and 7104 elements (including 48 triangular elements - T3 in Nastran nomenclature). The second one (Figure 5b) consists of 20353 nodes, 20616 elements (48 of triangular shape -T3). Both meshes are meth to be involved during the stage of comparison strain to acceleration measurements, but further on in text only the relaxed mesh is referred to. The target of numerical modal analysis was set up to 10 first mode shapes. Preliminary FE model was developed with the assumption of the same parameters for each of the pile guides, upper and lower braces. The computation results are presented in Table 1. It can be observed that double modes occur (i.e. having the same natural frequencies but different mode shapes) It is due to the symmetry and identical values of the moments of inertia. Components of the tripod were manufactured from the aluminum sheet produced accordingly to the Polish Standard PN-87/H-92741.02. It defines the bidirectional thickness deviation and the chemical composition ([%] of Si, Fe, Cu, Mn, Mg, Zn, and Al). Small differences around nominal identical design values were introduced into the FE model material properties individually for each particular braces and pile guides. The modified FE model yielded differences in natural frequency values although the modal density of the structure remain high and the modes are closely spaced (Table 5). The FE model with modified parameters was used in the pretest analysis.

### 3.3 Pretest analysis for sensor number and location definition

From developed FE-model of a tripod the components structural modes were derived with their corresponding frequencies by solving the FE-model with NASTRAN solver. In order to become a FE-model that, when used in simulation, behaves in the same way as the real structure in real life (and this is the goal), some changes may have to be made to the FE-model [6].

Table 1. Mode shapes and frequencies acquired during numerical modal analysis before parameters separation.

$\omega_1 = 62.9\text{Hz}$ 	$\omega_2 = 62.9\text{Hz}$ 
$\omega_3 = 104.1\text{Hz}$ 	$\omega_4 = 104.1\text{Hz}$ 
$\omega_5 = 221.2\text{Hz}$ 	$\omega_6 = 252.6\text{Hz}$ 
$\omega_7 = 252.6\text{Hz}$ 	$\omega_8 = 262.1\text{Hz}$ 
$\omega_9 = 284.2\text{Hz}$ 	$\omega_{10} = 284.2\text{Hz}$ 

The (modal) differences between the FE-model and the real structure, will be analyzed in section 5 by using correlation tools. The FE-model's modes calculated were used to define the most optimal measurement/test set-up. In the test-setup the set of measuring points and a set of excitation points was defined. Pre-Test analysis defines the optimal locations of these measurement and excitation points based on the FE-modes. The objective is to use the FE-model's modal data to define the test-setup providing high quality test-data: excite the structure at the right DOF's and measure the vibrations at the right DOF's to capture as many real-structure modes as possible. Afterwards the test-data will be analyzed and the modes derived from measurements will be compared to the modes derived from FE Analysis in section 5 describing the correlation analysis.

Investigated structure within other project activity was instrumented with 45 optical strain sensors. It limited a potential location of acceleration sensors. Therefore in the pretest analysis the arbitrary selected locations of 55 acceleration measurement points were verified with the evaluation of the proposed excitation points (Figure 6).

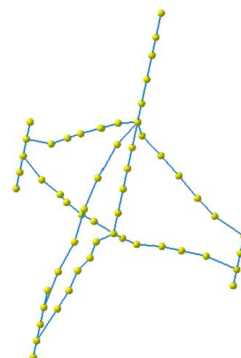


Figure 6 test wireframe with measurement points

To verify if there is no spatial aliasing in mode shapes captured with selected measurement points an AutoMAC analysis was carried out. An auto-MAC is in fact a MAC (Modal Assurance Criterion) with two times the same processing. More information about the MAC can be found in [4,5 6].

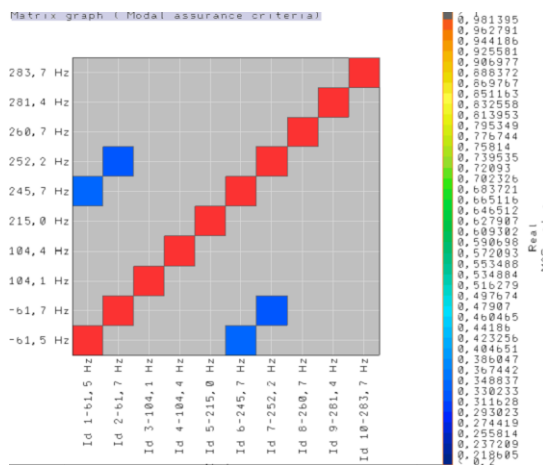


Figure7 AutoMAC matrix of the modes for selected measurement points

AutoMAC matrix from (Figure 7) shows which modes are correlated, only taking into account the displacement values of the wireframe nodes. In general, the MAC value is 1 if two mode shapes (modal vectors) are perfectly correlated, i.e. if they are identical up to a (complex) scaling factor. By definition, the diagonal elements of an AutoMAC matrix are 1 (a mode shape is perfectly correlated with itself). In the (Figure 7) it can be observed that values for the off the main diagonal of some modes are around 0,3. The low off-diagonal AutoMAC values indicate that the selected sensors are capable to distinguish the mode shapes from each other. In the next step the selection of excitation points were verified by means of Driving Point Residues analysis (Figure 8). Driving Point Residues (DRP) provide a means of analyzing which DOF is the most efficient in exciting the different modes. For each node of the candidate group, the driving point residue are calculated for all selected modes. For each node, the minimum and maximum values are presented as well as the average, and the weighted average values. The weighted average DPR is the product of the average DPR and the minimum DPR. The value provides global information on how well the modes of interest are excited by the different nodes from the group.

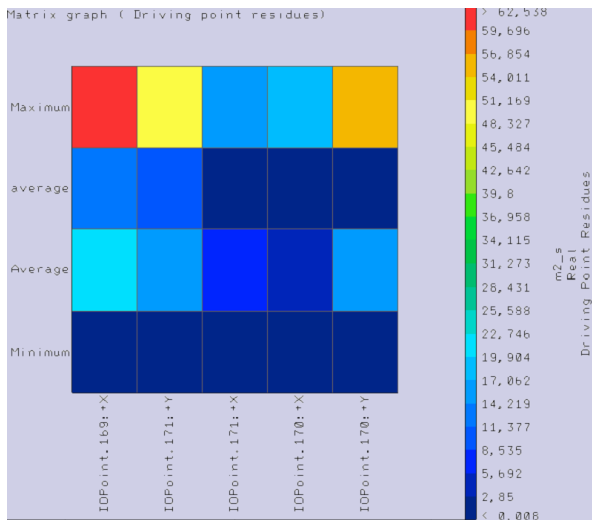


Figure 8 Driving Point Residues matrix

If an excitation in one DOF results in a very high response but for one mode only it isn't a very good candidate excitation point. So it is better to look at the average DPR (averaged over all the modes), or at average weighted DPR. Based on the Driving Point Residues analysis two excitation points selection (169 and 171) were confirmed to excite high response.

#### 4 EXPERIMENTAL MODAL ANALYSIS

Following the numerical modelling and pre-test analysis the experimental campaign was planned and implemented. It was done by means of experimental modal analysis with Multiple Input Multiple Output approach.

##### 4.1 Experimental setup

Tripod aluminum model was underslung by means of elastic cord fixed to the top of the model to provide a free-free boundary condition.

Lateral stiffness of the cord is considerably lower than longitudinal. It is expected then not to constrain the bending mode shape displacements of the central column. Structure was excited with two electrodynamic shakers attached to the pile guides through the mechanical impedance sensors for driving point Frequency Response Function measurement (Figure 9).

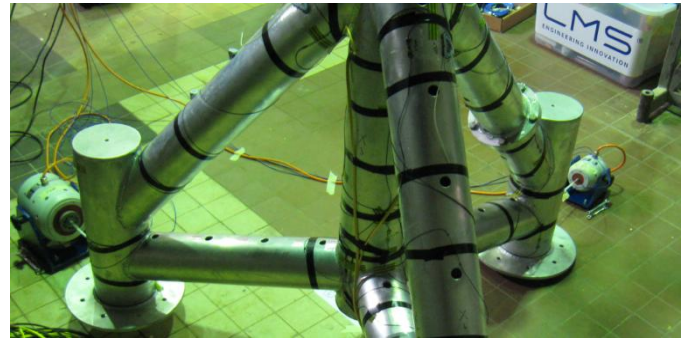


Figure 9 Electrodynamic shakers attached to the hanging tripod model.

Burst random excitation signal was used within the bandwidth of 0-1024 [Hz]. Shear piezoelectric tri-axial accelerometers were used to acquire the response signals. Dense grid of measurement points was developed with five measurement points defined on each of the subcomponents for adequate capturing the mode shapes. To avoid sensors' mass loading effect [1], [2], [3] only five sensors were used in a single test run. Global model was developed by merging partial models developed on particular sets of measurements.

##### 4.2 Measurement results

Measurement campaign comprised of 17 measurement runs, with 5 sensors per run covering in total 55 measurement points (Figure 6). It was verified that structure satisfies the modal analysis method assumptions as linearity and Maxwell's reciprocity theorem.

Reciprocity of Frequency Response Functions  $h$  means that measuring the response at Degree Of Freedom (DOF)  $i$  while exciting at DOF  $j$  is the same as measuring the response at DOF  $j$  while exciting at DOF  $i$  [4]. This is expressed mathematically in equation (1):

$$h_{ij}(\omega) = h_{ji}(\omega) \tag{1}$$

Response for excitation from shaker one measured at shaker two overlaps with response measured at shaker one from excitation from shaker two (Figure 10).

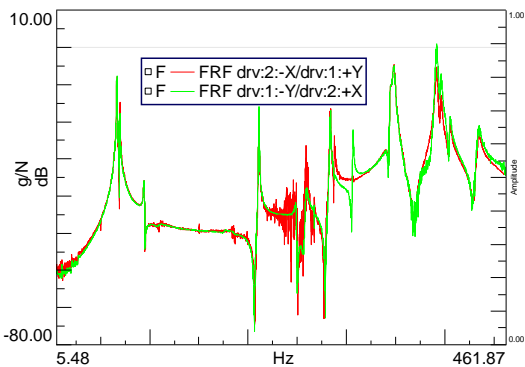


Figure 10 Verification of Maxwell's reciprocity theorem

Structure is characterized by a high modal density with numerous modes closely spaced within investigated bandwidth up to 400 [Hz] as presented on Figure 11.

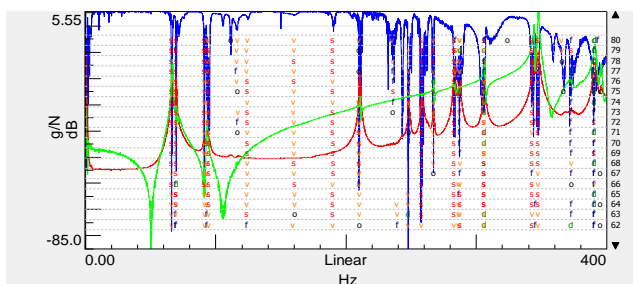


Figure 11 Example of the stabilization diagram showing potential natural frequencies of the object

4.3 Estimation of the modal model parameters

Estimation of the modal model parameters yielded 15 natural frequencies with corresponding damping coefficients. As presented in Table 2.

Table 2. Natural frequencies and damping ratios for identified experimental modes.

Mode No	Frequency [Hz]	Damping [%]
1	66,12	0,19
2	69,26	0,13
3	91,22	0,24
4	93,39	0,15
5	94,85	0,32
6	210,20	0,02
7	247,99	0,00
8	258,03	0,13
9	267,11	0,03
10	283,03	0,09
11	287,43	0,07
12	306,11	0,09
13	342,93	0,15
14	347,80	0,13
15	390,35	0,17

Data in Table 2 confirms the adequate identification of the natural frequencies on the stabilization diagram and presence of closely spaced modes. Structure is lightly damped and thus sensitive to the additional measurement equipment influence onto measured quantities. To verify the correctness of the modes estimation a mode shapes were compared by means of Auto Modal Assurance Criterion (Figure 12) [5].

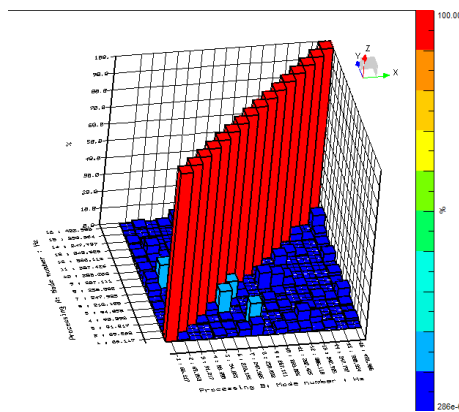


Figure 12 Auto Modal Assurance Criterion of the estimated mode shapes

MAC values for corresponding modes should be near 100 % meaning the linear relationship exists between the two vectors. MAC off main diagonal terms are small (near zero) as the particular modes modal vectors turn out to be linearly independent. Estimated mode shapes for natural frequencies are presented in (Table 3)

Table 3. Estimated mode shapes for natural frequencies

$\omega_1 = 66.1\text{Hz}$	$\omega_2 = 69.26\text{Hz}$
$\omega_3 = 91.22\text{Hz}$	$\omega_4 = 93.39\text{Hz}$
$\omega_5 = 94.85\text{Hz}$	$\omega_6 = 210.20\text{Hz}$
$\omega_7 = 247.99\text{Hz}$	$\omega_8 = 258.03\text{Hz}$
$\omega_9 = 267.11\text{Hz}$	$\omega_{10} = 283.03\text{Hz}$

### 5 CORRELATION AND VALIDATION ANALYSIS

Finite Element Method model and Experimental Modal Analysis models can be compared for the assessment of the consistency of the results produces from both methods. Natural frequencies and mode shapes are subject of assessment. Both models need to be correlated to implement a validation analysis.

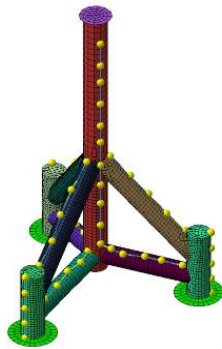


Figure 13 Measurement grid and the Finite Element mesh nodes correlation. Yellow bulbs denote measurement points assigned to nodes of the mesh for mode shape comparison.

Correlated geometries (Figure 13) of the experimental and numerical models allow to transfer modal vectors both measured and computed to the correlated coordinate systems. Transferred vectors were compared by means of MAC criterion as presented in (Table 4). Test model is the reference model and the FE model is the verification model.

Table 4. Comparison of the differences between natural frequencies of the Verification numerical model and Reference experimental model.

VER mode Id1	FEM Freq	EF mode Id	Freq2	MAC Value	Freq2-Freq1 (Hz)	Freq2-Freq1 (% of Freq1)
1	61,5	1	66,1	0,822	4,64	7,6
2	61,7	2	69,3	0,864	7,6	12,3
4	104,4	3	91,2	0,225	-13,14	-12,6
4	104,4	4	93,4	0,248	-10,97	-10,5
4	104,4	5	94,9	0,276	-9,5	-9,1
5	215	6	210,2	0,6	-4,83	-2,2
6	245,7	7	248	0,378	2,31	0,9
7	252,2	8	258	0,49	5,85	2,3
8	260,7	9	267,1	0,138	6,45	2,5
9	281,4	10	283	0,508	1,58	0,6
10	283,7	11	287,4	0,602	3,77	1,3

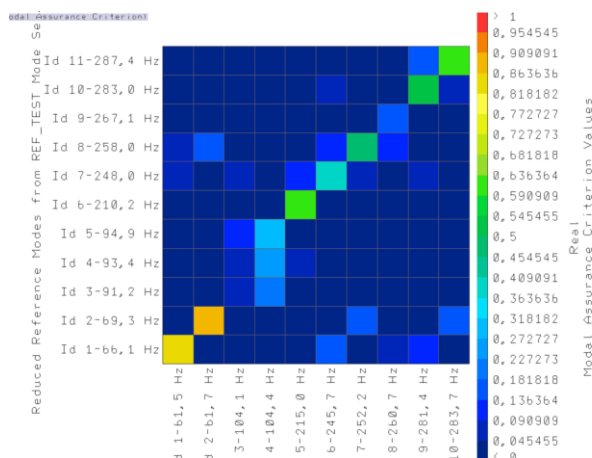


Figure 14 Modal Assurance Criterion evaluating discrepancies between numerical (verification) and experimental (reference) models.

MAC matrix (Figure 14) reveals two modes which are coinciding in terms of frequency but have weaker consistency of the mode shapes. These are namely central column (tower) bending mode around 100 Hz and the twist modes of pile guides at around 260 Hz.

In the vibration test the suspension of the structure was an elastic cord attached to the top flange of the central column of the tripod. Lateral stiffness which is the direction of the bending mode displacement is significantly smaller than a stiffness in the longitudinal direction of the cord. It is planned configuration with the objective not to constrain the lateral Degree of Freedom. As it was confirmed both in simulation and measurement the compression modes of the tripod (along the longitudinal direction of the central column) are not present within the investigated frequency bandwidth. It could be explained by higher stiffness of the cylindrical beam in longitudinal direction. The implemented test setup has a drawback as entire weight of the structure is effectively carried by the central column. This causes a pretension of the structure under the gravity load and constrains to certain extent the bending mode degree of freedom. Moreover the shakers attached to the pile guides were standing on the ground which implements further constrain to the investigated mode. Small difference in the observed values of the natural frequencies obtained from test and simulation clearly indicate the existence of the mode. Solution of this problem could be a repeating of the test with different supporting method releasing the introduced pretension. In particular, an attractive option would be supporting entire tripod on the large rubber bloc under the bottom of the central column.

In the second case of satisfactory correspondence of mode frequencies is the torsional mode of the pile guides at around 260 Hz. Top view of the mode both in test and FE display the rotary degree of freedom as the main component of the displacement. Accelerometers used in the measurement are capable of capturing translational degree of freedom displacements, no rotational ones (Figure 15).

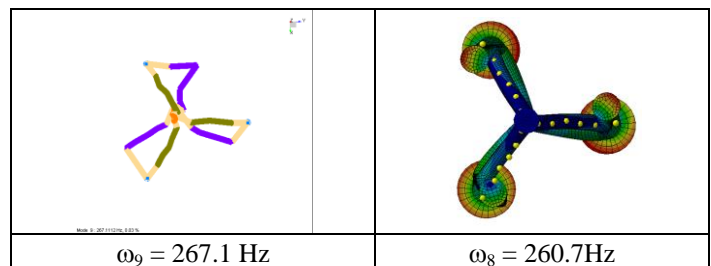


Figure 15 Experimental (left) and numerical (right) torsional mode shape - top view.

Improvement of the results could be achieved by measurement of more than one line on the pile guide cylindrical beam. Measuring the additional lines on the circumference of the cylinder would yield information on the rotation as the combination of the translational displacements.

### 6 PRELIMINARY NUMERICAL MODEL UPDATING

Estimated experimental modal model was applied in two ways: to identify structural dynamics properties described by means of the modal model parameters and as a reference data for the numerical model updating.

6.1 Sensitivity analysis

Sensitivity analysis allow to identify the numerical model parameters most influential on the natural frequencies values and mode shapes. The model parameters were being defined as design variables to analyze the frequency (1) and mode (2) sensitivities. To establish such relation Taylor’s series expansion is used. In case of FE model rate of change in the resonance frequencies and mode shapes can be quantified as follows [7]:

$$\frac{\partial \omega_i}{\partial q} = \frac{1}{2m_i} [\Phi]_i^T \left( -\omega_i \frac{\partial [M]}{\partial q} + \frac{1}{\omega_i} \frac{\partial [K]}{\partial q} \right) [\Phi]_i \tag{1}$$

$$\frac{\partial [\Phi]_i}{\partial q} = -\frac{1}{2m_i} [\Phi]_i^T \frac{\partial [M]}{\partial q} [\Phi]_i [\Phi]_i + \sum \frac{1}{\omega_i^2 - \omega_k^2} \frac{1}{m_k} [\Phi]_k^T \left( -\omega_i^2 \frac{\partial [M]}{\partial q} + \frac{\partial [K]}{\partial q} \right) [\Phi]_i [\Phi]_k \tag{2}$$

where:

- [M] – mass matrix,
- [K] – stiffness matrix,
- [Φ] – mode shape vector (subscript r – undamped),
- m – modal mass,
- ω - resonance frequency (subscript r – damped),
- q – tested parameter.

Geometry of the tripod components (thickness of the cylinder walls (T) and Young modulus of the material) were selected. Outcomes of the frequency sensitivity analysis are presented on the (Figure 16).

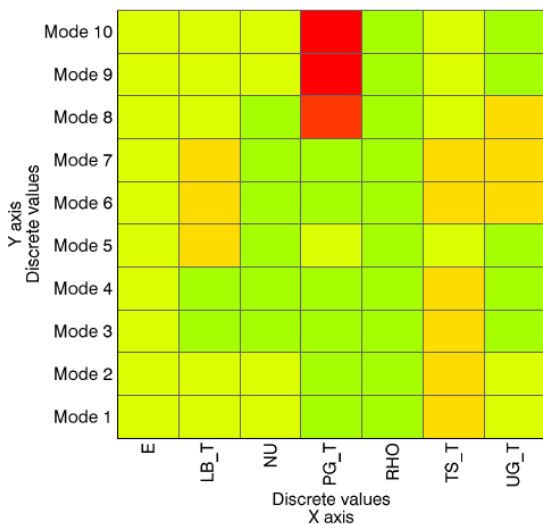


Figure 16 Normalized mode frequency sensitivities matrix plot representing most influential design variables (Young modulus, Poisson’s ratio, thickness and mass density) onto the particular mode frequency values

As it can be seen, change of modes 8 to 10 depends on the same parameter. Additionally, the analysis shows that Young modulus, Poisson’s ratio, and mass density play negligible role on influencing natural frequencies. The dependence in

case of modes 8-10 is caused by assigning the same parameters to group for: mud-mats (1 property), pile sleeves (1 property), lower diagonal braces (1 property), upper diagonal braces (1 property), central column (1 property). A solution for this problem is separation of the structural members properties. Each of tripled structural members now gained their distinctive property, except mud-mats which were never considered as the influencing structural members. Instead of initial 7 parameters the model now consists of 10 parameters. This change allows to alter not only the inertial property but also shifting the positioning of the principal axes of inertia. A new sensitivity matrix shows (Figure 17) evidently that now the FE model could be updated with assumption of non-homogeneity of the material.

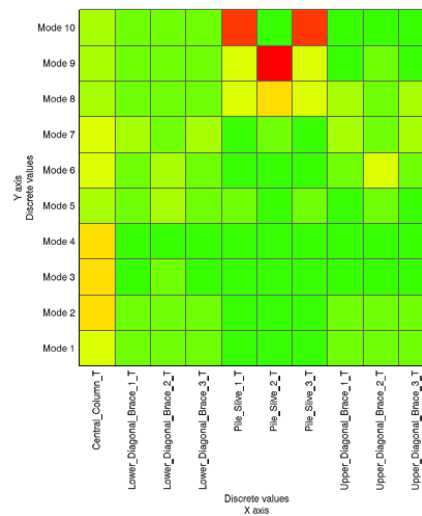


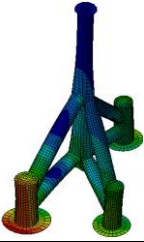
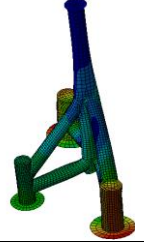
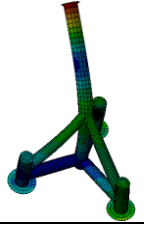
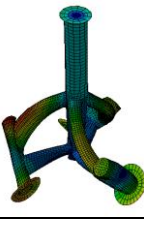
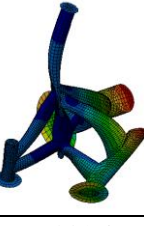
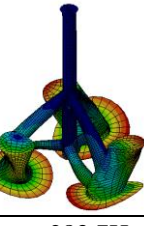
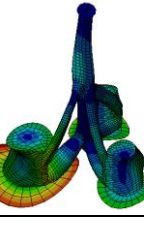
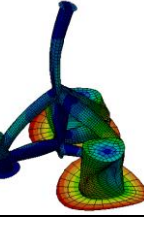
Figure 17 New sensitivity matrix

Parameters of mud-mats, Young modules, Poisson’s ratios, and the density of material were excluded from sensitivity analysis as not relevant. Nonsymmetrical properties of the test structure can be caused for example by structural changes in rolled aluminum after welding, i.e. due to change in structure of the material, or an inaccuracy during manufacturing stage. The effect of parameters separation is presented in (Table 5). It is now evident that previously paired modes -due to the equal inertial properties of initial FE model - (Table 1), after change are now separated (Table 5).

ACKNOWLEDGMENTS

This research was supported by a Polish National Research and Development Center under the project PBS1/A6/8/2012 “AQUILO”. The authors of this work gratefully acknowledge support for this research Marie Curie Initial Training Network project No. 309395 “MARE-WINT” within 7th European Community Framework Programme provided by the EU. This research was supported in part by PL-Grid Infrastructure and computations were performed at CI TASK Supercomputing Centre in Gdansk, Poland.

Table 5. Mode shapes and frequencies acquired during numerical modal analysis after parameters separation.

$\omega_1 = 61.5\text{Hz}$ 	$\omega_2 = 61.7\text{Hz}$ 
$\omega_3 = 104.1\text{Hz}$ 	$\omega_4 = 104.7\text{Hz}$ 
$\omega_5 = 215\text{Hz}$ 	$\omega_6 = 245.7\text{Hz}$ 
$\omega_7 = 252.2\text{Hz}$ 	$\omega_8 = 260.7\text{Hz}$ 
$\omega_9 = 281.4\text{Hz}$ 	$\omega_{10} = 283.7\text{Hz}$ 

- [6] LMS International, *The LMS Theory and Background Book—Analysis and Design*, Manual of Virtual.Lab Revision 11, LMS International, (2011),
- [7] Fox, R., L., Kapoor, M., P., *Rates of Change of Eigenvectors and Eigenvalues*, *AIAA Journal*, Vol. 6, 1968, Pages 2426-2429.
- [8] Lozano-Minguez, E., Kolios, A. J., and Brennan, F. P., *Multi-Criteria Assessment of Offshore Wind Turbine Support Structures*, *Renewable Energy*, 36(11) (2011), pp. 2831-2837

## REFERENCES

- [1] Warren, C., Niezrecki, C., Avitabile, P., *Comparison of FRF Measurements and Mode Shapes Determined using Optically Image Based, Laser, and Accelerometer Measurements*, *Mechanical Systems and Signal Processing*, Volume 25, Issue 6, August 2011, Pages 2191–2202
- [2] Bi, S., Ren, J., Wang, W., *Elimination of Transducer Mass Loading Effects in Shaker Modal Testing*, *Mechanical Systems and Signal Processing*, Volume 38, Issue 2, 20 July 2013, Pages 265–275
- [3] Cakar, O., and Sanliturk, K., *Elimination of Transducer Mass Loading Effects from Frequency Response Functions*, *Mechanical Systems and Signal Processing*, Volume 38, Issue 2, 20 July 2013, Pages 265–275
- [4] LMS International, *The LMS Theory and Background Book—Analysis and Design*, Manual of Test.Lab Revision 5, LMS International, (2005),
- [5] Allemang, Randall J. *The modal assurance criterion—twenty years of use and abuse*, *Sound and Vibration* 37.8 (2003): 14-23.